# Scattering of <sup>11</sup>Be around the Coulomb barrier

L. Acosta\*, M.A.G. Álvarez<sup>†,\*\*</sup>, M.V. Andrés<sup>†</sup>, M.J.G. Borge <sup>‡</sup>, M. Cortés<sup>‡</sup>, J.M. Espino<sup>†</sup>, D. Galaviz<sup>‡</sup>, J. Gómez-Camacho<sup>†,\*\*</sup>, A. Maira<sup>‡</sup>, I. Martel<sup>\*</sup>, A.M. Moro<sup>†</sup>, I. Mukha<sup>†</sup>, F. Pérez-Bernal<sup>\*</sup>, E. Reillo<sup>‡</sup>, K. Rusek<sup>§</sup>, A.M. Sánchez-Benítez<sup>\*</sup> and O. Tengblad<sup>‡</sup>

\*Departamento de Física Aplicada, Universidad de Huelva, E-21071 Huelva, Spain †Departamento de Física Atómica Molecular y Nuclear, Universidad de Sevilla, E-41080 Sevilla \*\*Centro Nacional de Aceleradores, Universidad de Sevilla-CSIC-Junta de Andalucía, E-41092 Sevilla, Spain

‡Instituto de Estructura de la Materia, CSIC, Madrid, E-28006 Madrid, Spain §The Andrzej Soltan Institute for Nuclear Studies, 00-681 Warsaw, Poland

#### Abstract.

Preliminary results on the  $^{11}\text{Be}+^{120}\text{Sn}$  quasielastic scattering as well as the  $^{11}\text{Be}\to^{10}\text{Be}+n$  breakup channel are presented in this work. The angular distributions of these channels were measured at REX-ISOLDE-CERN. The accuracy and angular range of the presented results provide stronger constrains to the theoretical interpretation than existing published results. We compare these new data with coupled-channel (CC) and continuum-discretized coupled-channel (CDCC) calculations. The role played by transfer and breakup channels in the elastic scattering is discussed.

**Keywords:** <sup>11</sup>Be, quasielastic, coupled-channel, halo nuclei, Coulomb barrier **PACS:** 25.45.De 25.70.Mn 24.10.Eq 25.60.-t

### INTRODUCTION

The  $^{11}$ Be is a halo nucleus composed of a  $^{10}$ Be core and a weakly bound neutron. This nuclide has a half life of 13.8 s and a separation energy for one neutron of 504(6) keV. The only bound excited state ( $J^{\pi}=1/2^{-}$ ) lies at 320 keV with a strong coupling to the ground state ( $J^{\pi}=1/2^{+}$ ) by the fastest known E1 transitions. Due to its loosely bound structure, coupling to the continuum should play an important role in near barrier scattering with heavy targets. Therefore the  $^{11}$ Be nucleus is an interesting case to study the dynamics of nuclear haloes at Coulomb barrier energies [1, 2].

Another important issue is the role played by the highly deformed <sup>10</sup>Be core on the scattering cross sections [3]. Accurate data on <sup>11</sup>Be scattering are needed to study these effects. Presently the only results published are from one experiment performed in RIKEN [4, 5]. Unfortunately, the angular distributions presented in the mentioned analysis suffer of large experimental uncertainties, and elastic and other reaction channels could not be studied separately.

Aiming to improve the experimental situation we have recently performed measurements of <sup>11</sup>Be scattered on <sup>120</sup>Sn at 32 MeV (lab). The experiment was performed at the REX-ISOLDE facility at CERN (Geneva), using a detection system that covered a wide angular range.

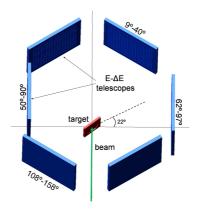


**FIGURE 1.** Schematic representation of the experimental setup. Downstream and upstream detectors are placed symmetrically with respect to the beam direction. The target was tilted  $22^{\circ}$  in order to cover angles around  $90^{\circ}$  with the lateral telescopes.

#### **EXPERIMENT**

The experiment IS444 was performed using a post-accelerated  $^{11}$ Be beam at the energy of 2.91 MeV/u and a  $^{120}$ Sn target, in order to study the scattering around the Coulomb barrier. The experimental setup consisted of an hexagonal configuration with 6 telescope detectors in E- $\Delta$ E configuration, surrounding the target. Each telescope was made up of two silicon detectors: a thin ( $\Delta$ E) Double-Sided Silicon Strip Detector (DSSSD) with a thickness of 40  $\mu$ m and divided in 16 strips in each side; and a PAD silicon detector (E) with a thickness of 500  $\mu$ m. If we impose coincidences between strips in the front and back side (mutually perpendicular) of a DSSSD, we get what we call a "pixel" (16x16 in total). A schematic representation of the experimental setup is shown in Fig. 1. The target was tilted 68° with respect to the beam axis in order to allow the detection in the telescopes placed around 90°.

Due to the low intensity of the beam we used a thick (3.5 mg/cm²) tin target. This fact limited the energy resolution of our detection system to about 350 keV, spoiling the possibility of resolving the excitation of  $^{11}$ Be to the  $1/2^-$  first excited state (inelastic channel). However the resolution was good enough to identify  $^{10}$ Be fragments resulting from breakup  $^{11}$ Be  $\rightarrow$   $^{10}$ Be + n for the angular range (15°-38°). Therefore, we could separate the quasielastic channel (elastic+inelastic) from the breakup channel in the mentioned range, by means of the analysis made pixel-by-pixel. Using pixels instead of full strips, it was possible to separate the breakup event from quasielastic ones, as the angular spread and kinematical effects are reduced. The difference between a full strip and one pixel is shown in the  $\Delta$ E-E $_t$  spectra of the Fig. 2 at  $\theta_{lab} \sim 34^\circ$ .

For the  $\theta_{lab}$  range (52°-86°) it was not possible to separate the breakup from the quasielastic channel, because only part of the events had enough energy to go through the  $\Delta E$  detector. In this case, we integrated the sum of quasielastic and breakup channels. The accumulated statistics registered in telescopes at  $\theta_{lab}$  larger than 90° was too small to produce cross section data.

The measured angular distribution was normalized to Rutherford cross sections using the elastic scattering data of a <sup>12</sup>C beam impinging in the same <sup>120</sup>Sn target at 27 MeV.

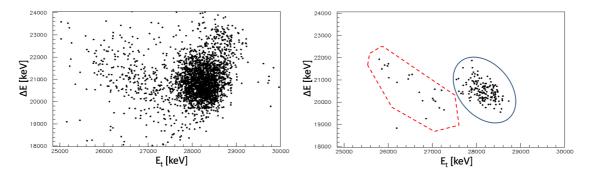


**FIGURE 2.** Differences between full strip and pixel.  $\Delta E$ - $E_t$  spectra around 34° (lab). The spectrum on the left shows the elastic+inelastic+breakup scattering for a full strip, the separation between channels seems not to be possible. On the right panel, one pixel from that strip is shown. In this case, we can observe the separation between quasielastic (solid polygon) and breakup (dashed polygon) channels.

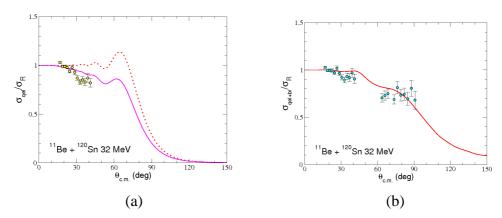


**FIGURE 3.** Comparison of experimental results and calculations. (a) Quasielastic scattering vs.  $\theta_{c.m.}$  (dots) and CC calculations (dotted and solid lines). (b) Quasielastic+breakup channel vs.  $\theta_{c.m.}$  (dots) and a CDCC calculation (solid line). See text for details.

## RESULTS

The angular distribution obtained for quasielastic channel is shown in the Fig. 3a. The overall shape is similar to the angular distributions measured previously in the elastic scattering of the weakly bound <sup>6</sup>He on <sup>208</sup>Pb [6, 7]. However, the deviation from the Rutherford cross section at forward angles is much more pronounced in the case of <sup>11</sup>Be scattering. In order to reproduce the data shape we performed two CC calculations. The first (dotted line) includes the first excited state and two resonant states (1.78 MeV and 3.41 MeV). The strong absorption at very forward angles is not well reproduced. The second calculation includes, as proposed in [8, 9] two fictitious dipole states (*p*-states) located at excitation energy of 0.55 MeV, just above the breakup threshold, with spins  $1/2^-$  and  $3/2^-$ . These states are intended to represent the low-lying dipole strength for the <sup>11</sup>Be continuum. With these parameters the agreement between calculation and data results is acceptable. Further details of this calculations can be consulted in [10].

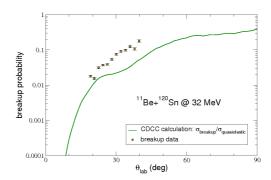


**FIGURE 4.** Breakup probability, defined as the ratio between the breakup and quasielastic events. Comparison between experimental results and CDCC calculation.

In Fig 3b we show preliminary results obtained for the quasielastic+breakup channel (dots). We include a CDCC calculation (solid line) generated with the potentials for the different channels taken from [11, 12, 13]. These new results show a good agreement with the calculation and even with the data presented in [5] at 46 MeV.

Fig. 4 shows the ratio between the breakup and the quasielastic events, shown in Fig. 3a. The solid line is the prediction of the CDCC calculation shown in Fig. 3b. In this case, the calculation underestimates the data. This discrepancy could be due to the contribution of higher partial waves of the <sup>11</sup>Be continuum, or the contribution of other channels not included in this calculation, such as the one-neutron transfer to the target.

### **ACKNOWLEDGMENTS**

This work has been supported by the Spanish CICYT, under the project FPA2007-62170, the Spanish Council of Science and Education (MEC) under the research grants FINURA (FPA2007-63074), CPAN (CSD 2007-00042), the DGICYT under the project FPA2006-13807-c02-01 and Consolider-Ingenio CSD-2007-00042. L.A. acknowledges financial support by XI Plan Propio de Investigación from the Universidad de Huelva.

#### REFERENCES

- 1. L.F. Canto et al., Phys. Rev. C52 R2848 (1995).
- 2. K. Yabana, Y. Ogawa and Y. Suzuki, Phys. Rev. C58 2403 (1998).
- 3. N.C Summers et al., *Phys. Rev.* C74 014606 1-12 (2006).
- 4. M. Mazzocco et al., Eur. Phys. J. A52 295 (2006).
- 5. M. Mazzocco et al., Eur. Phys. J. Special Topics 150 37 (2007).
- 6. O.R. Kakuee et al., *Nucl. Phys.* **A765** 294 (2006).
- 7. A.M. Sánchez-Benítez et al., Nucl. Phys. A803 30 (2008).
- 8. M. Takashina, S. Takagi and Y. Sakuragi, *Phys. Rev.* C67 037601 (2003).
- 9. D.J. Howell, J.A. Tostevin and J.S. Al-Khalili, J. Phys. G31 S1881 (2005).
- 10. L. Acosta et al., Eur. Phys. J. A (accepted).
- 11. J.J. Kolata et al., Phys. Rev. C69 047601 (2004).
- 12. A.J. Koning and J.P. Delaroche, Nucl. Phys. A713 247 (2003).
- 13. P. Capel, G. Goldstein and D. Baye, Phys. Rev. C70 064605 (2004).